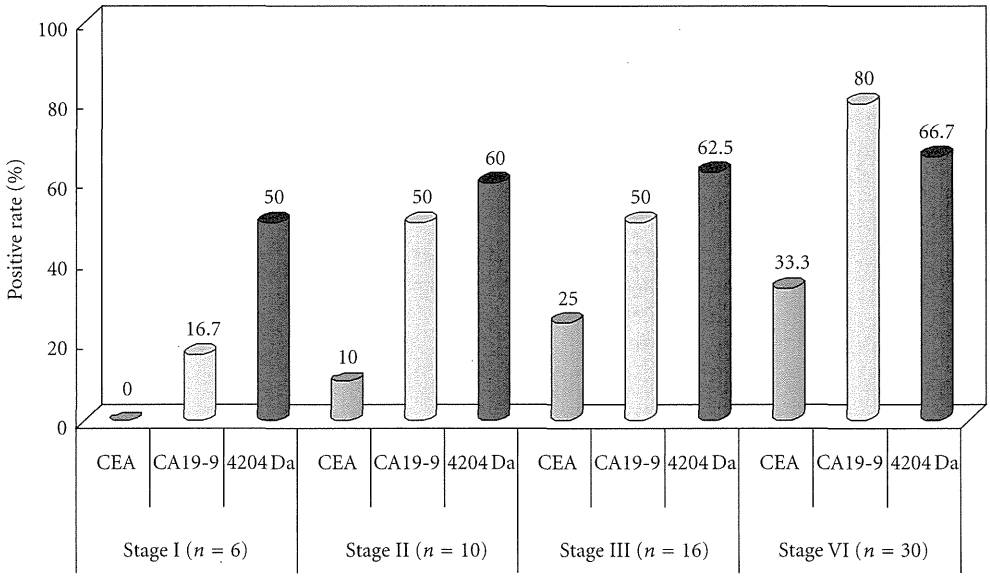

FIGURE 4: Positive rates of detection of the 4204 Da peptide, CEA, and CA19-9 in each UICC stage.

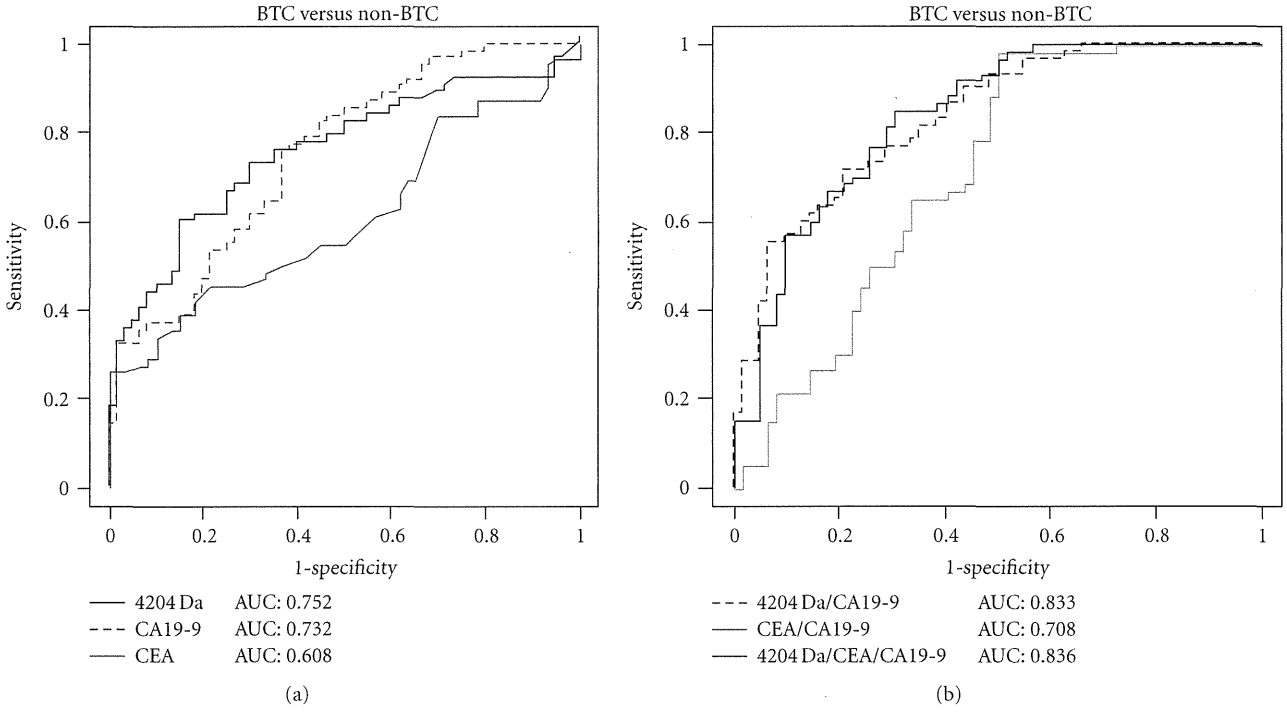

FIGURE 5: ROC analyses of the performance of the 4204 Da peptide, CA19-9, and CEA. (a) AUC was 0.752 for 4204 Da, 0.732 for CA19-9, and 0.608 for CEA. (b) AUC was 0.833 for 4204 Da + CA19-9, 0.708 for CA19-9 + CEA, and 0.836 for 4204 Da + CEA + CA19-9.

Biliary tract cancer is a particularly lethal malignancy with a mean 1-year survival of only 6% for unresectable cases [4]. The lack of a sensitive and specific biomarker for early detection of BTC is one of the reasons for this limited survival. Cholangiocarcinoma often grows along the bile duct without forming a mass, and thus is often missed in CT and ultrasound. Serum biomarkers with satisfactory sensitivity and specificity are likely to be beneficial in the clinical management of this malignancy. There have been previous attempts to discover biomarkers for cholangiocarcinoma. Scarlett et al. conducted proteomic profiling of sera from cases of cholangiocarcinoma using SELDI-TOF MS and found that a serum peptide corresponding to a 4463 m/z peak had superior discriminatory ability to CA19-9 and CEA, but did not identify the peak [16]. More recently, a membrane protein enrichment strategy coupled with ^{18}O labeling-based

quantitative proteomics was used to identify proteins that are highly expressed in cholangiocarcinoma tissues [17]. Golgi membrane protein, annexin IV, and epidermal growth factor were proposed as candidate markers. However, their diagnostic roles at the serum level were not described.

CEA and CA19-9 are tumor markers for BTC with average sensitivity and specificity for detecting cholangiocarcinoma of 51% and 88%, respectively, for CEA, and 71% and 78%, respectively, for CA19-9 [7]. In the present study, the sensitivities of CEA, CA19-9, and the 4204 Da peptide for detection of all BTC cases were 50%, 61.3%, and 75.8%, respectively. It was of note that the sensitivity of 4204 Da in stages I and II patients was far greater than those of the conventional markers and that serum 4204 Da peptide levels were elevated in 79% of cases in which both CA19-9 and CEA were within their reference intervals. These findings suggest that this novel peptide is complementary to conventional markers in diagnosis of BTC. This is supported by the greater AUC with the combination of CEA, CA19-9, and the 4204 Da peptide, compared to individual AUCs.

The result obtained in identification of the 4204 Da peptide was unexpected. The peptide was identified as a fragment of prothrombin, which makes it unlikely that the fragment originated from cancer tissues. It is possible that production of the fragment occurred in the cancer-tissue microenvironment. Alternatively, the 4204 Da peptide might have been generated ex vivo by undefined degradative proteases during the clotting process [18]. The exact mechanism for production of the 4204 Da peptide remains to be clarified. We also note that intrahepatic cholangiocellular carcinoma, extrahepatic cholangiocellular carcinoma, and gall bladder carcinoma were analyzed together as BTCs in the present study. Separate analyses of these diseases on a larger scale are needed to discover biomarkers that are more specific for each form of BTC. Also, antibody-based verification will be necessary to further confirm the findings obtained in this study. Bile samples may also be an alternative for discovery of disease markers leaking from the biliary tree [19].

Abbreviations

AU:	Arbitrary unit
BTC:	Biliary tract cancer
MALDI-TOF MS:	Matrix-associated laser desorption ionization time-of-flight mass spectrometry
CEA:	Carcinoembryonic antigen
CA19-9:	Carbon hydrate antigen 19.9
ROC:	Receiver operation characteristic
AUC:	Area under the curve.

Authors' Contribution

These authors contributed equally to the work.

Acknowledgments

The authors thank Fumie Iida and Manami Miura for their technical support.

References

[1] S. A. Khan, H. C. Thomas, B. R. Davidson, and S. D. Taylor-Robinson, "Cholangiocarcinoma," *Lancet*, vol. 366, no. 9493, pp. 1303–1314, 2005.

[2] T. Patel, "Cholangiocarcinoma," *Nature Clinical Practice Gastroenterology and Hepatology*, vol. 3, no. 1, pp. 33–42, 2006.

[3] Y. Shaib and H. B. El-Serag, "The epidemiology of cholangiocarcinoma," *Seminars in Liver Disease*, vol. 24, no. 2, pp. 115–125, 2004.

[4] W. R. Jarnagin and M. Shoup, "Surgical management of cholangiocarcinoma," *Seminars in Liver Disease*, vol. 24, no. 2, pp. 189–199, 2004.

[5] G. J. Gores, "Cholangiocarcinoma: current concepts and insights," *Hepatology*, vol. 37, no. 5, pp. 961–969, 2003.

[6] E. M. Abu-Hamda and T. H. Baron, "Endoscopic management of cholangiocarcinoma," *Seminars in Liver Disease*, vol. 24, no. 2, pp. 165–175, 2004.

[7] O. Nehls, M. Gregor, and B. Klump, "Serum and bile markers for cholangiocarcinoma," *Seminars in Liver Disease*, vol. 24, no. 2, pp. 139–154, 2004.

[8] H. J. Issaq, T. P. Conrads, D. A. Prieto, R. Tirumalai, and T. D. Veenstra, "SELDI-TOF MS for diagnostic proteomics," *Analytical Chemistry*, vol. 75, no. 7, pp. 148A–155A, 2003.

[9] F. Nomura, T. Tomonaga, K. Sogawa et al., "Identification of novel and downregulated biomarkers for alcoholism by surface enhanced laser desorption/ionization-mass spectrometry," *Proteomics*, vol. 4, no. 4, pp. 1187–1194, 2004.

[10] S. Takano, H. Yoshitomi, A. Togawa et al., "Apolipoprotein C-1 maintains cell survival by preventing from apoptosis in pancreatic cancer cells," *Oncogene*, vol. 27, no. 20, pp. 2810–2822, 2008.

[11] J. Villanueva, J. Philip, D. Entenberg et al., "Serum peptide profiling by magnetic particle-assisted, automated sample processing and MALDI-TOF mass spectrometry," *Analytical Chemistry*, vol. 76, no. 6, pp. 1560–1570, 2004.

[12] K. Sogawa, M. Satoh, Y. Kodera, T. Tomonaga, M. Iyo, and F. Nomura, "A search for novel markers of alcohol abuse using magnetic beads and MALDI-TOF/TOF mass spectrometry," *Proteomics*, vol. 3, no. 7, pp. 821–828, 2009.

[13] L. H. Sobin and I. D. Fleming, "TNM classification of malignant tumors, 5th edition (1997)," *Union Internationale Contre le Cancer and American Joint Committee on Cancer*, vol. 80, no. 9, pp. 1803–1804, 1997.

[14] H. Umemura, M. Nezu, Y. Kodera et al., "Effects of the time intervals between venipuncture and serum preparation for serum peptidome analysis by matrix-assisted laser desorption/ionization time-of-flight mass spectrometry," *Clinica Chimica Acta*, vol. 406, no. 1-2, pp. 179–180, 2009.

[15] B. Seliger, S. P. Dressler, E. Wang et al., "Combined analysis of transcriptome and proteome data as a tool for the identification of candidate biomarkers in renal cell carcinoma," *Proteomics*, vol. 9, no. 6, pp. 1567–1581, 2009.

[16] C. J. Scarlett, A. J. Saxby, A. Nielsen et al., "Proteomic profiling of cholangiocarcinoma: diagnostic potential of SELDI-TOF MS in malignant bile duct stricture," *Hepatology*, vol. 44, no. 3, pp. 658–666, 2006.

[17] T. Z. Kristiansen, H. C. Harsha, M. Grønborg, A. Maitra, and A. Pandey, "Differential membrane proteomics using 18O-labeling to identify biomarkers for cholangiocarcinoma," *Journal of Proteome Research*, vol. 7, no. 11, pp. 4670–4677, 2008.

[18] J. Villanueva, D. R. Shaffer, J. Philip et al., "Differential exoprotease activities confer tumor-specific serum peptidome

patterns," *Journal of Clinical Investigation*, vol. 116, no. 1, pp. 271–284, 2006.

[19] A. Farina, J. M. Dumonceau, and P. Lescuyer, "Proteomic analysis of human bile and potential applications for cancer diagnosis," *Expert Review of Proteomics*, vol. 6, no. 3, pp. 285–301, 2009.

Human Pathology (2012) 43, 1282–1288

ELSEVIER

Human
PATHOLOGY

www.elsevier.com/locate/humpath

Original contribution

Prohibitin in squamous cell carcinoma of the lung: its expression and possible clinical significance☆

Feng Guo MD, PhD[a,b], Kenzo Hiroshima MD, PhD[b,*], Di Wu PhD[b], Mamoru Satoh PhD[c], Mayinuer Abulazi MD, PhD[c], Ichiro Yoshino MD, PhD[d], Takeshi Tomonaga MD, PhD[e], Fumio Nomura MD, PhD[c], Yukio Nakatani MD, PhD[a]

[a]*Department of Diagnostic Pathology, Chiba University Graduate School of Medicine, Chiba 260-8670, Japan*
[b]*Department of Pathology, Tokyo Women's Medical University Yachiyo Medical Center, Chiba 276-8524, Japan*
[c]*Department of Molecular Diagnosis, Chiba University Graduate School of Medicine, Chiba 260-8670, Japan*
[d]*Department of Thoracic Surgery, Chiba University Graduate School of Medicine, Chiba 260-8670, Japan*
[e]*Laboratory of Proteome Research, National Institute of Biomedical Innovation, Osaka 567-0085, Japan*

Received 23 June 2011; revised 21 October 2011; accepted 21 October 2011

Keywords:
Lung squamous cell carcinoma;
Fluorescent 2-D differential gel electrophoresis;
Prohibitin;
Immunohistochemical analysis;
Prognostic significance

Summary rohibitin is localized to mitochondria where it might have a role in the maintenance of mitochondrial function and protection against senescence. In this study, we show that prohibitin is up-regulated in lung squamous cell carcinoma tissues compared with adjacent normal tissues using agarose 2-dimensional differential gel electrophoresis and immunoblotting. Prohibitin expression was further evaluated by immunohistochemistry. We statistically analyzed the association of prohibitin expression with clinicopathologic indicators in 78 patients with lung squamous cell carcinoma. Our data suggested that prohibitin expression was positively correlated with the International Union Against Cancer (UICC) classification of tumor grade ($P < .001$), pathologic stage ($P < .001$), tumor size ($P = .01$), and lymph node metastasis ($P = .004$). Furthermore, we found that prohibitin expression was an independent prognostic indicator ($P = .037$) for overall survival of patients with lung squamous cell carcinoma by multivariate analysis using the Cox regression method. These findings may encourage further studies investigating prohibitin function in lung squamous cell carcinoma.

1. Introduction

Lung cancer is a leading cause of cancer death in both men and women worldwide. The prognosis of this disease remains unfavorable. Non–small cell lung cancer accounts for almost 80% of lung cancers, of which 60% are squamous cell carcinoma (SqCC) [1]. In general, pathologic TNM stage is the most reliable prognostic factor for predicting the outcome of treatment. The 5-year survival rates range from 77% for stage IA tumors to 23% in stage IIIA disease. Although adjuvant chemotherapy has recently been established as a standard of care for resected stage II to III non–small cell lung cancer, the overall absolute 5-year survival benefit from this approach does not exceed 5%. Therefore, a deeper understanding of the molecular mechanisms involved in the pathogenesis and progression of lung cancer may lead to new and more effective strategies for early detection to improve patient survival rates [2].

☆ Disclosure/Conflict of Interest: The authors declare no conflict of interest.

* Corresponding author.
E-mail address: kenzo@tymc.twmu.ac.jp (K. Hiroshima).

0046-8177/$ – see front matter © 2012 Elsevier Inc. All rights reserved.
doi:10.1016/j.humpath.2011.10.006

Proteomic technologies have been used to explore the pathogenesis of tumors and to screen for early diagnostic markers and potential drug targets. In recent years, a new emerging technology for proteomic analysis is fluorescent 2-dimensional differential gel electrophoresis (2D-DIGE). This technique appears to have the advantage of good sensitivity, high reproducibility, and a wide dynamic range. We have previously identified several novel proteins with altered expression in primary esophageal cancer and hepatocellular cancer using a combination of 2-dimensional gel electrophoresis (2-DE) and 2D-DIGE [3,4]. This technique is a new powerful tool for identifying disease-related proteins in lung cancer.

We analyzed primary SqCC tissues and adjacent normal tissues using agarose 2D-DIGE and identified a large number of proteins with consistent differential expression, one of which was prohibitin (PHB). Western blot and immunohistochemistry (IHC) demonstrated that PHB was significantly overexpressed in many lung SqCC tissues. Moreover, we found that PHB is an independent prognostic factor for patients with lung SqCC. Recently, new PHB-targeting anticancer agents have been tested in clinical trials [5]. Thus, development of a simple and reliable method to measure the level of PHB could be helpful in selecting patients who might qualify for these new PHB therapies.

2. Materials and methods

2.1. Agarose 2D-DIGE and immunoblotting

2.1.1. Tissue specimens and preparation

Tissues from 10 cases of primary lung SqCC were resected surgically without any neoadjuvant therapy. All excised tissues were immediately placed in liquid nitrogen and stored at −80°C until analysis.

2.1.2. Protein extraction

Frozen tissue samples were solubilized in lysis buffer (30 mmol/L Tris-HCl [pH 8.5], 7 mol/L urea, 2 mol/L thiourea, 4% wt/vol 3-[(3-cholamidopropyl)dimethylammonio]-1-propanesulfonate (CHAPS)) containing protease inhibitor mixture (Complete; Roche, Mannheim, Germany) using a Polytron homogenizer (Kinematica, Littau-Luzern, Switzerland) after centrifugation (100 000×*g*) for 1 hour at 4°C. The total protein concentration was determined with the Bio-Rad Protein Assay Kit (Bio-Rad, Tokyo, Japan).

2.1.3. Agarose 2D-DIGE

Protein labeling was performed using the CyDye DIGE Fluores developed for fluorescence 2D-DIGE technology (Amersham Biosciences, Buckinghamshire, UK) according to the manufacturer's recommended protocol. Each noncancer sample was labeled with Cy3, and each cancer sample was labeled with Cy5. An internal standard, created by pooling aliquots of all the samples and labeling with Cy2, was used to normalize protein abundance measurements across multiple gels in each experiment. These samples were mixed before isoelectric focusing on agarose isoelectric focusing, followed by second-dimension sodium dodecyl sulfate–polyacrylamide gel electrophoresis. The second dimensional gel was scanned using a fluorescence image scanner, Typhoon 9400 (GE Healthcare UK Ltd, Little Chalfont, UK), and was analyzed using the image analyzing software DeCyder (GE Healthcare UK Ltd). Non-labeled 150 μg whole-tissue lysates (containing equal volumes of 2× sample buffer) were separated by 2-DE. The 2-DE gel was conducted as described [3]. Different protein spots were cut out of the conventional agarose 2-DE gel and were subjected to in gel digestion, followed by identification by Matrix Assisted Laser Desorption/Ionization Time of Flight Mass Spectrometry (MALDI-TOF MS) as we described before [3].

2.1.4. Immunoblotting

Protein extracts were separated by electrophoresis on a 10% to 20% polyacrylamide gradient gel (Bio-Rad, Hercules, CA). Mouse monoclonal anti-PHB (Abcam, Cambridge, UK) and goat anti–β-actin antibody (Santa Cruz Biotechnology, Santa Cruz, CA) diluted 1:500 in phosphate-buffered saline were used as primary antibodies. Goat antimouse immunoglobulin G and rabbit antigoat immunoglobulin G conjugated to horseradish peroxidase (Cappel, West Chester, PA), diluted 1:1000 in blocking buffer, were used as secondary antibodies. Antigens on the membrane were detected by ECL detection reagents (GE Healthcare UK Ltd). The intensity of each band was measured using National Institutes of Health (NIH) Image.

2.2. Immunohistochemical analysis and statistical analysis

2.2.1. Immunohistochemistry

The staining procedure is described as follows: archival blocks were collected from 78 patients with primary lung SqCC who were diagnosed between January 1, 1995, and December 31, 2004, at Chiba University Hospital, Japan. The survival of patients was followed until death or until December 31, 2009. The median follow-up time was 56 months (range, 7-100 months). Tissue sections (4 μm thick) were cut from all samples and deparaffinized and mounted on precoated slides. Sections were treated with 0.1% hydrogen peroxide for 15 minutes to block endogenous peroxidase activity, and epitopes were retrieved by autoclaving at 121°C for 15 minutes in 0.02 mol/L citrate buffer at pH 6.0. Slides were incubated with primary PHB antibody (1:200) at 4°C overnight. We used human heart tissue as a positive control. Visualization of immunoreactivity was achieved using 3,3′-diaminobenzidine tetrahydrochloride as a chromogen. Immunoreactivity was evaluated by 3 investigators (F.G., K.H., and Y.N.).

2.2.2. Evaluation of IHC results

We evaluated PHB immunoreactivity according to the method of Tsao et al [6], with slight modifications [7]. The

PHB immunoreactivity of tumors was assessed by estimating staining intensity and the approximate proportion of positively stained tumor cells. Staining results were classified as follows: low expression was indicated by no or weak staining, or staining in less than 40% of tumor cells regardless of the intensity; high expression was indicated by moderate-to-strong staining in at least 40% of tumor cells.

2.2.3. Statistical analysis

Correlation of PHB and clinicopathologic indicators of lung SqCC was determined using the χ^2 test. The Kaplan-Meier method was used to estimate overall survival (OS) and disease-free survival (DFS). Patient survival time was calculated from the date of surgery until the time of death (OS) or first local or distant recurrence (DFS). The log-rank test was used to examine statistical significance. Multivariate analysis was determined by the Cox proportional hazards model. The results were considered significant when $P < .05$ was obtained.

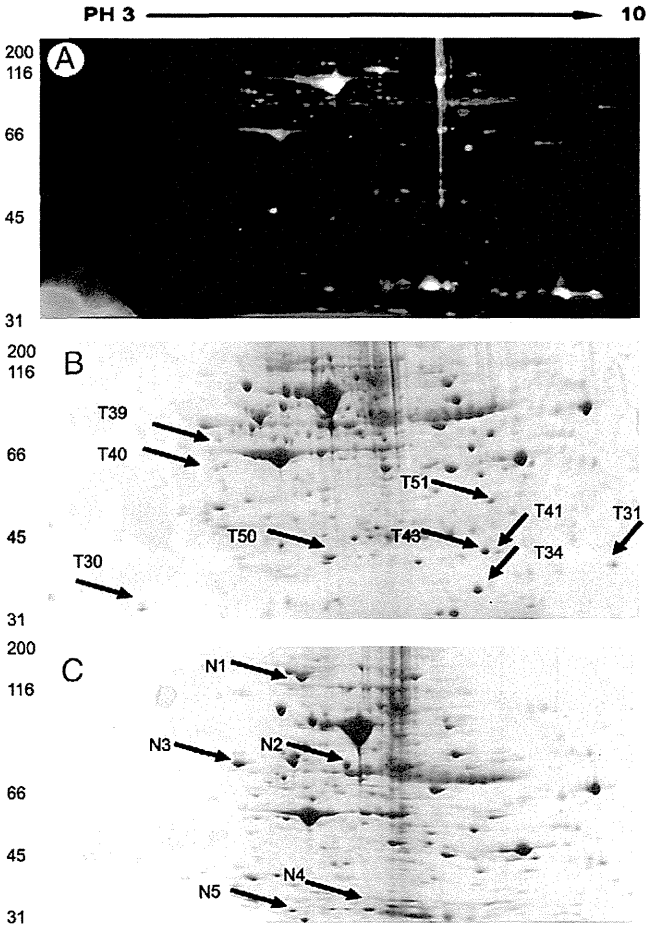

Fig. 1 Proteomic analysis of lung SqCC tissues using 2D-DIGE. A, Increased protein spots in tumor tissues are displayed as red (cy5), and decreased protein spots in tumor tissues are displayed as green (cy3). B and C, Conventional agarose 2-DE patterns were visualized by Coomassie brilliant blue staining. Proteins of primary lung SqCC (B) and adjacent normal tissue (C) were separated. The protein spots cut from this gel were identified by MALDI-TOF MS.

3. Results

3.1. Identification of proteins with altered expression in human lung SqCC tissue

Proteins were prepared as described, and labeled proteins were mixed and separated by agarose 2D-DIGE (Fig. 1A). The protein spots were detected and quantitated with DeCyder imaging analysis software, and statistical analysis was performed for 10 gels. The fluorescence volumes of 36 spots increased and 37 spots decreased in cancer tissues compared with adjacent normal tissue (Student t test, $P < .05$). To identify these proteins, 150 μg of whole-tissue lysates was separated by 2-DE and protein was visualized by Coomassie brilliant blue staining (Fig. 1B and C). By MALDI-TOF MS, 51 (36 proteins) spots were identified from 63 spots. Among these proteins, 31 were up-regulated and 5 were down-regulated in cancer tissues. The up-regulated proteins included peroxiredoxin (T43), Nm23 (T34), vimentin (T39), annexin (T50), and aldolase A (T51), whose expression has been previously reported to be altered in lung SqCC [8,9].

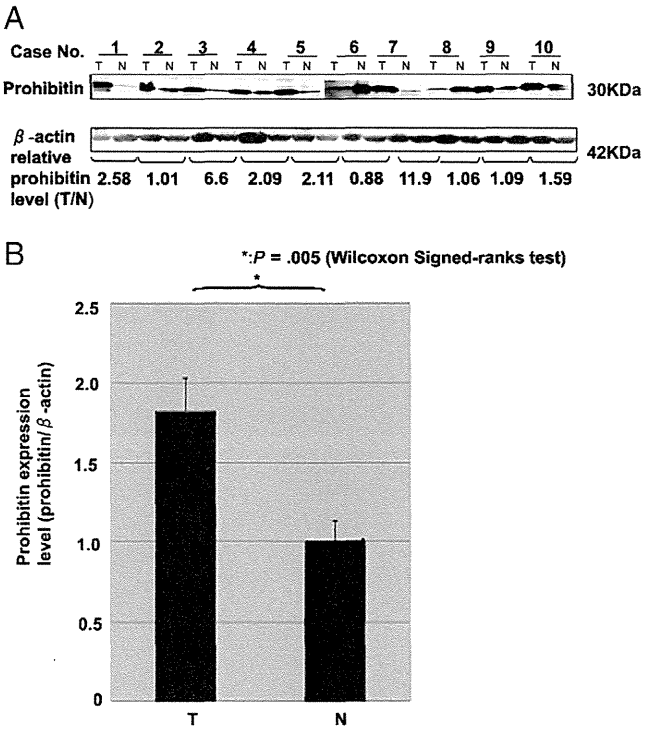

Fig. 2 Up-regulation of PHB in primary lung SqCC. Protein lysates prepared from 10 matched samples of tumor (T) and adjacent nontumor tissue (N) were resolved on a 10% to 20% polyacrylamide gel and immunoblotted with anti-PHB antibody and with a β-actin antibody as a loading control. The intensity of each band was measured with NIH Image, and the relative PHB protein levels between tumors and nontumor tissue were normalized to β-actin. A, The expression of PHB significantly increased in tumor tissues. B, The difference of PHB expression between T and N was assessed by the Wilcoxon signed ranks test for unpaired values.

Expression of other proteins such as PHB (T30), transgelin (T41), p21-Arc (T31), and tropomyosin (T40) was also shown to be up-regulated in other cancer tissues either by 2-DE or other methods [10,11]. The down-regulated proteins included periplakin (N1), heat shock protein (HSP)70 (N2), CK18 (N3), keratin1 (N4), and HSP27 (N5) [3,12,13]. We chose to focus on PHB. In 10 paired cases, spot T30 (PHB) was unequivocally displayed in seven tumor cases but was almost undetectable in the 2-DE maps of normal tissues, and it has not been extensively studied in human primary lung SqCC. To confirm the differential expression of PHB between tumor and normal tissue, we used Western blotting. Eight of 10 cases showed up-regulated expression of PHB ($P = .005$) (Fig. 2A and B).

3.2. IHC and clinicopathologic relevance of PHB in SqCC cases

Only faint PHB immunoreactivity was observed in normal bronchial epithelia and alveolar pneumocytes. We found that PHB was mainly expressed in the cytoplasm of tumor cells (Fig. 3), and 85% of cases (66/78) were positive for PHB staining. The expression of PHB was divided into 2 groups as described in the "Materials and methods." Of the 78 tumors examined, 33 tumors showed low expression and 45 tumors showed high expression of PHB. The results are shown in Table 1. High expression of PHB was positively correlated with the International Union Against Cancer (UICC) classification of tumor grade ($P < .001$), pathologic stage ($P < .001$), tumor size ($P = .01$), and lymph node metastasis ($P = .004$). However, expression of PHB did not relate to other biological indicators such as pleural involvement, lymphatic invasion, or vascular invasion ($P > .05$).

3.3. PHB expression is correlated with patient survival

Patients who had high expression of PHB had lower OS and DFS (Fig. 4A and B). To identify independent predictors for survival, univariate and multivariate Cox

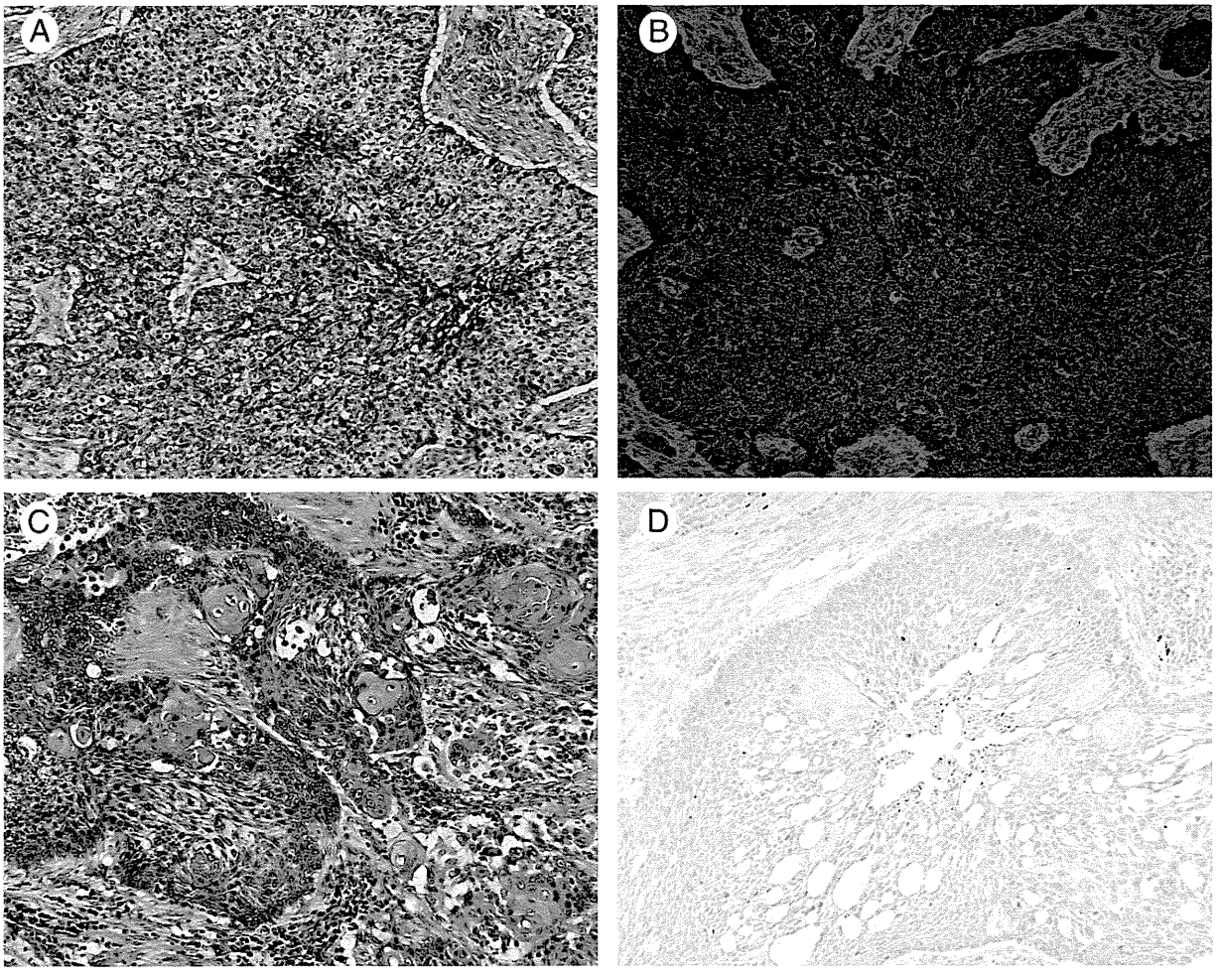

Fig. 3 Immunostaining of PHB in lung SqCC. A, Poorly differentiated SqCC (hematoxylin and eosin [HE] stain). B, Immunostaining for PHB in the same sample as panel A. Note the moderate-to-strong cytoplasmic positivity in most of the tumor cells. C, Well-differentiated SqCC (HE stain). D, Immunostaining for PHB in the same sample as panel C. Note the mostly negative immunostaining in the tumor cells.

Table 1 Correlation of PHB expression with clinicopathologic parameters

Clinicopathologic characteristics	PHB expression [a]		*P**
	Low	High	
Differentiation [b]			<.001*
G1 (17) + G2 (36)	30	23	
G3 (25)	3	22	
LN metastatic			.004*
Positive (32)	6	26	
Negative (46)	27	19	
Tumor diameter (cm)			.01*
>3 (46)	14	32	
≦3 (32)	19	13	
Pleural involvement [c]			.8
Positive (23)	11	12	
Negative (55)	24	31	
Pathologic stage			<.001*
Stage I (41)	25	16	
Stage II (21)	7	14	
Stages III-IV (16)	1	15	
Lymphatic invasion			.2
Positive (18)	6	12	
Negative (60)	30	30	
Vascular invasion			.05
Positive (15)	3	12	
Negative (63)	30	33	

* χ^2 Test, $P < .05$.

[a] Low, no or weak staining, or staining in less than 40% of tumor cells regardless of the intensity. High, moderate-to-strong staining in at least 40% of tumor cells.

[b] G1, well differentiated; G2, moderately differentiated; G3, poorly differentiated.

[c] Positive was defined as P1, P2, and P3, Negative was defined as P0.

regression analyses were performed. In the univariate analysis (Table 2), significant factors predicting decreased OS were expression of PHB ($P = .001$), lymph node metastasis ($P = .01$), pathologic stage ($P = .002$), lymphatic invasion ($P = .009$), and vascular invasion ($P = .0009$). Factors associated with decreased DFS were PHB expression ($P = .034$), lymph node metastasis ($P = .03$), and pathologic stage ($P = .0006$) (Table 2). Factors with $P < .05$ in both OS and DFS in univariate analysis were entered into a stepwise multivariate proportional model. As a result, PHB ($P = .037$) was an independent prognostic factor as significant as pathologic stage ($P = .031$) in the OS of patients. Pathologic stage was the only independent variable associated with DFS (Table 3).

4. Discussion

PHB is a ubiquitous 30-kDa conserved protein, which is found in a wide range of organisms such as bacteria, plants, yeast, and mammals [14]. PHB has been shown to localize to mitochondria, but nuclear localization of PHB, recently reported in different cell types, is controversial [15].

At the gene level, several studies have suggested that PHB has a potential role as a tumor suppressor [16-18]. When messenger RNA of PHB was microinjected into HeLa cells, PHB was found to block cell entry into the S phase of the cell division cycle. At the protein level, PHB may function as a tumor suppressor through binding to the retinoblastoma (RB) family of proteins and repressing E2F-mediated transcription, which plays a major role in controlling mammalian cell cycle progression [18].

Conflicting experimental data are reported concerning the role of PHB in tumorigenesis. PHB is required in the control of RAS-induced RAF-MEK-ERK activation, which is a central signaling pathway involved in cell growth and malignant transformation in many cell types [16]. Thus, PHB expression should be permissive to tumor growth. Recent studies have indicated that mitochondrial PHB might function as a chaperone similar to HSP60 and mortalin [19], Therefore, PHB may play important roles in the aging process and tumorigenesis through effects on the stability of newly encoded mitochondrial proteins and the subsequent assembly of respiratory chain complexes. It is conceivable that overexpression of PHB may extend the life span of tumor cells, which could be a critical step in the establishment of tumorigenic clones in the early stage of carcinogenesis [20].

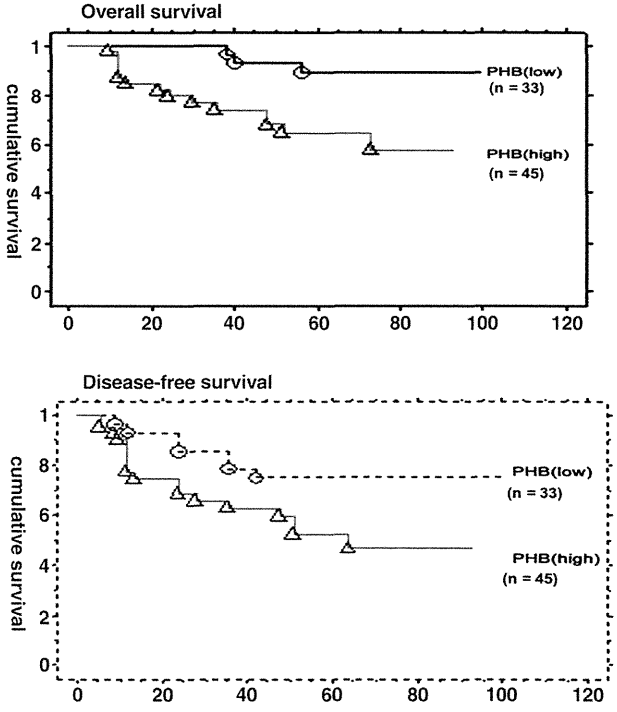

Fig. 4 Kaplan-Meier analysis of PHB expression in relation to clinical outcome. Significance of PHB expression in association with patient survival was assessed using a log-rank test. High PHB expression significantly correlated with decreased OS (A) and DFS (B).

Table 2 Univariate analysis of predictive factors for OS and DFS

Factor	OS		DFS	
	5-y (MST;mo)	*P*	5-y (MST;mo)	*P*
PHB expression		.001 *		.034 *
Low (33)	89.4%		75.0%	
High (45)	57.6%		56.0%	
LN metastasis		.01 *		.03 *
Negative (46)	83.3%		83.8%	
Positive (32)	50.5%		57.9%	
Pathologic stage		.002 *		.0006 *
Stage I (41)	84.0%		85.0%	
Stage II (21)	63.2%		70.1%	
Stages III-IV (16)	40.6%		22.3%	
Grade		.22		.08
G1 (17) + G2 (36)	74.2%		79.9%	
G3 (25)	62.6%		63.8%	
Tumor diameter		.11		.48
≦ 3cm (32)	82.0%		66.0%	
> 3cm (46)	69.5%		59.6%	
Pleural invasion		.14		.29
Negative (55)	80.0%		78.0%	
Positive (23)	63.5%		65.4%	
Lymphatic invasion		.009 *		.11
Negative (60)	76.5%		77.0%	
Positive (18)	36.3%		56.7%	
Vascular invasion		.009 *		.13
Negative (63)	79.9%		77.2%	
Positive (15)	36.2%		49.5%	

Abbreviation: MST, median survival.
* Log-rank test, $P < .05$.

Using a powerful proteomic technique, agarose 2D-DIGE, combined with immunoblotting and IHC, we found that PHB was overexpressed in lung SqCC tissues compared with noncancerous regions. This result is consistent with prior studies using transformed cells or cancer cell lines from the uterine cervix, endometrium, liver, breast, and bladder [7,21-24]. Ummanni et al [15] reported a significant up-regulation of PHB in prostate cancer compared with benign prostatic hyperplasia. Wang et al [25] and Ryu et al [26] showed that PHB was overexpressed in gastric cancer tissues compared with noncancerous regions by 2-DE and proposed that PHB was a biomarker for gastric cancer. Meanwhile, Jupe et al [27] observed that all breast cancer cell lines overexpressed PHB messenger RNA and protein, and they proposed that PHB overexpression might be caused by a mutation in the 3′-untranslated region. However, this mutation has not been observed in other human tumors so far. The possibility remains that a mutation occurs in other regions of the gene in other tissues that have not yet been studied and may play a role in the cancer development.

There have been a few studies on the expression of PHB in lung cancers. One recent study using a shot-gun proteomics strategy showed that PHB is a candidate protein for a biomarker of lung SqCC [28]. A few other proteomics analysis studies focused on the correlation between altered expression of proteins and drug resistance in lung cancer cell lines [29,30]. Increased expression of PHB was correlated, either positively or inversely, with drug resistance. These apparently contradictory results may be related to the different cell lines and/or drugs used in these studies.

In our IHC study of 78 lung SqCC cases, significantly increased expression of PHB was detected in high-grade SqCC tissues compared with low-grade cancer tissues, implying that PHB overexpression may be an important event in the tumorigenesis of lung SqCC. We also found that overexpression of PHB was correlated with lymph node metastasis, pathologic stage, and tumor size. The PHB gene in cancer cells was activated after c-myc up-regulation in response to oxidative stress, and it was proposed that PHB may defend against oxidative injury, suppress apoptosis in mammalian cells, and promote survival of cancer cells [20]. It is possible that PHB may act as a progressor by protecting tumor cells from oxidative stress when the tumor increases its volume or metastasizes to the lymph nodes.

Although PHB overexpression is associated with short DFS for patients with esophageal SqCC and bladder cancer [31,32], there have been no studies demonstrating any prognostic value of PHB expression in patients with lung SqCC. Analysis of our data revealed that PHB overexpression was significantly related to poor prognosis in patients with lung SqCC. Using univariate and multivariate Cox regression analyses, we demonstrated that overexpression of PHB was an independent risk factor for worse prognosis in patients with lung SqCC. The IHC of PHB could provide clinically useful prognostic information in cases of lung SqCC.

In summary, we showed that PHB was overexpressed in lung SqCC tissues compared with noncancerous tissues. Patients with PHB overexpression had a significantly lower OS rate and DFS rate than those with low PHB expression.

Table 3 Multivariate analysis of predictive factors for OS and DFS

Factor	Relative risk	95% confidence intervals		*P*
		Lower	Upper	
OS				
PHB expression Low *vs* high	0.294	0.093	0.931	.037 *
Pathologic stage: I-II *vs* III-IV	0.382	0.159	0.92	.031 *
DFS				
PHB expression Low *vs* high	0.851	0.278	2.605	.77
Pathologic stage: I-II *vs* III-IV	0.179	0.063	0.507	.001 *

* Cox proportional hazards model, $P < .05$.

Therefore, PHB might be another avenue to explore for targeted therapy for human lung SqCC.

Acknowledgments

We thank Mrs Yoko Hata for her technical assistance.

References

[1] Hammerschmidt S, Wirtz H. Lung cancer: current diagnosis and treatment. Dtsch Arztebl Int 2009;106:809-18.
[2] Ioannidis G, Georgoulias V, Souglakos J. How close are we to customizing chemotherapy in early non–small cell lung cancer? Ther Adv Med Oncol 2011;3:185-205.
[3] Nishimori T, Tomonaga T, Matsushita K. Proteomic analysis of primary esophageal squamous cell carcinoma reveals downregulation of a cell adhesion protein, periplakin. Proteomics 2006;6: 1011-8.
[4] Seimiya M, Tomonaga T, Matsushita K, et al. Identification of novel immunohistochemical tumor markers for primary hepatocellular carcinoma; clathrin heavy chain and formiminotransferase cyclodeaminase. Hepatology 2008;48:519-30.
[5] Mishra S, Murphy LC, Nyomba BL, Murphy LJ. Prohibitin: a potential target for new therapeutics. Trends Mol Med 2005;11: 192-7.
[6] Tsao MS, Liu N, Chen JR, et al. Different expression of Met/hepatocyte growth factor receptor in subtypes of non–small cell lung cancer. Lung Cancer 1998;20:1-16.
[7] Tsai HW, Chow NH, Lin CP, Chan SH, Chou CY, Ho CL. The significance of prohibitin and c-met/hepatocye growth factor receptor in the progression of cervical adenocarcinoma. Hum Pathol 2006;37: 198-204.
[8] Deng B, Ye N, Luo G, Chen X, Wang Y. Proteomics analysis of stage-specific proteins expressed in human squamous cell lung carcinoma tissues. Cancer Biomarker 2005;1:279-86.
[9] Hu BQ, Xiao GM, Luo Y, Zhou SL, Xi XP, Ouyang QC. Screening of molecular markers of lung squamous cell carcinoma by microarrays. Zhonghua Zhong liu Za Zhi 2004;26:660-3.
[10] Qi Y, Chiu JF, Wang L, Kwong DL, He QY. Comparative proteomic analysis of esophageal squamous cell carcinoma. Proteomics 2005;5: 2960-71.
[11] Sewell DA, Yuan CX, Robertson E. Proteomic signatures in laryngeal squamous cell Carcinoma. ORL J Otorhinalaryngol Relat Spec 2007;69:77-84.
[12] Vercoutter-Edouart AS, Lemoine J, Le Bourthis X. Proteomic analysis reveals that 14-3-3 sigma is down-regulated in human breast cancer cells. Cancer Res 2001;61:76-80.
[13] Chow SN, Chen RJ, Chen CH, et al. Analysis of protein profiles in human epithelial ovarian cancer tissues by proteomic technology. Eur J Gynaeclo Oncol 2010;31:55-62.
[14] Nueu MJ, Stewart DA, Walker L, et al. Prohibitin, an evolutionarily conserved intracellular protein that block DNA synthesis in normal fibroblasts and HeLa cells. Mol cell Biol 1991;11:1372-81.
[15] Ummanni R, Junker H, Zimmermana U, et al. Prohibitin identified by proteomic analysis of prostate biopsies distinguished hyperplasia and cancer. Cancer Lett 2008;266:171-85.
[16] Rajalingam K, Wunder C, Brinkmann V, et al. Prohibitin is required for Ras-induced Raf-MEK-ERK activation and epithelial cell migration. Nat Cell Biol 2005;7:837-43.
[17] Wang S, Nath N, Adlam M, Chellappan S. Prohibitin, a potential tumor suppressor, interacts with RB and regulates E2F function. Oncogen 1999;18:3501-10.
[18] McClung JK, Jupe ER, Liu XT, Dell'Orco RT. Prohibitin: potential role in senescence development and tumor suppression. Exp Geronoto 1995;30:99-124.
[19] Crarnecka AM, Canpanella C, Zummo G, Gappello F. Mitochondrial chaperones in cancer: from molecular biology to clinical diagnostics. Cancer Biol Ther 2006;5:714-20.
[20] Coates PJ, Nenutil R, McGregor A, et al. Mammalian prohibitin proteins respond to mitochondrial stress and decrease during cellular senescence. Exp Cell Res 2001;265:262-73.
[21] Byrjasen I, Mose LP, Fey SJ, et al. Two-dimensional gel analysis of human endometrial proteins: characterization of protein with increased expression in hyperplasia and adenocarcinoma. Mol Hum Report 1999;8:748-56.
[22] Seow TK, Ong SE, Liang RC, et al. Two-dimensional electrophoresis map of the human hepatocellular carcinoma cell line, HCC-M, and identification of the separated protein by mass spectrometry. Electrophoresis 2000;21:1787-813.
[23] Williamis K, Chubb C, Hubermern E, Giometti CS. Analysis of differential protein expression in normal and neoplastic human breast epithelial cell lines. Electrophosis 1998;19:333-43.
[24] Asamoto M, Colens S. Prohibitin gene is over-expressed but not mutated in rat bladder carcinoma and cell lines. Cancer Lett 1994;83:201-7.
[25] Wang KJ, Wang RT, Zhang JZ. Identification of tumor marker using two-dimensional electrophoresis in gastric carcinoma. World J Gastroenterol 2004;10:2179-83.
[26] Ryu JW, Kim HJ, Lee YS, et al. The proteomics approach to find biomarkers in gastric cancer. Korean Med Sci 2003;18:505-9.
[27] Jupe ER, Liu XT, Kiehlbauch JL, McClung JK, Dell'Orco RT. Prohibitin in breast cancer cell lines: loss of antiproliferative activity is linked to 3′ untranslated region mutations. Cell Growth Differ 1996;7: 871-8.
[28] Nan Y, Yang S, Tian Y, et al. Analysis of the expression protein profiles of lung squamous carcinoma cell using shot-gun proteomics strategy. Med Oncol 2009;26:215-21.
[29] Li C, Xiao Z, Cheng Z, et al. Proteome analysis of human lung squamous carcinoma. Proteomics 2006;6:547-58.
[30] Patel N, Chatterjee SK, Vrbanac V, et al. Rescue of paclitaxel sensitivity by repression of prohibitin in drug-resistant cancer cells. Proc Natl Acad Sci 2010;107:2503-8.
[31] Wu TF, Wu H, Wang YW. Prohibitin in the pathogenesis of transitional cell bladder cancer. Anticancer Res 2007;27:895-900.
[32] Ren HZ, Wang JS, Pan GQ, et al. Increased expression of prohibitin and its relationship with poor prognosis in esophageal squamous cell carcinoma. Pathol Oncol Res 2010;16:515-22.

Hindawi Publishing Corporation
International Journal of Proteomics
Volume 2012, Article ID 623190, 12 pages
doi:10.1155/2012/623190

Research Article

The Application of a Three-Step Serum Proteome Analysis for the Discovery and Identification of Novel Biomarkers of Hepatocellular Carcinoma

Asako Kimura,[1] Kazuyuki Sogawa,[2] Mamoru Satoh,[1] Yoshio Kodera,[2,3] Osamu Yokosuka,[4] Takeshi Tomonaga,[1,5] and Fumio Nomura[1,2]

[1] *Department of Molercular Diagnosis, Graduate School of Medicine, Chiba University, Chiba 260-0856, Japan*
[2] *Clinical Proteomics Research Center, Chiba University Hospital, Chiba, Japan*
[3] *Laboratory of Biomolecular Dynamics, Department of Physics, Kitasato University School of Science, Kanagawa, Japan*
[4] *Department of Medicine and Clinical Oncology, Graduate School of Medicine, Chiba University, Chiba 260-0856, Japan*
[5] *Laboratory of Proteome Research, National Institute of Biomedical Innovation, Osaka, Japan*

Correspondence should be addressed to Fumio Nomura, fnomura@faculty.chiba-u.jp

Received 7 February 2012; Accepted 5 June 2012

Academic Editor: Dayan B. Goodenowe

The representative tumor markers for HCC, AFP, and PIVKA-II are not satisfactory in terms of sensitivity and specificity in the early diagnosis of HCC. In search for novel markers for HCC, three-step proteome analyses were carried out in serum samples obtained from 12 patients with HCC and 10 with LC. As a first step, serum samples were subjected to antibody-based immunoaffinity column system that simultaneously removes twelve of abundant serum proteins. The concentrated flow-through was then fractionated using reversed-phase HPLC. Proteins obtained in each fraction were separated by SDS-PAGE. Serum samples obtained from patient with HCC and with LC were analyzed in parallel and their protein expression patterns were compared. A total of 83 protein bands were found to be upregulated in HCC serum. All the protein bands, the intensity of which was different between HCC and LC groups, were identified. Among them, clusterin was most significantly overexpressed ($P = 0.023$). The overexpression of serum clusterin was confirmed by ELISA using another validation set of HCC samples. Furthermore, serum clusterin was elevated in 40% of HCC cases in which both AFP and PIVKA-II were within their cut-off values. These results suggested that clusterin is a potential novel serum marker for HCC.

1. Introduction

Hepatocellular carcinoma (HCC) is one of the most common cancers in the world and is a leading cause of death in many countries. Chronic infection by hepatitis B virus (HBV) or hepatitis C virus (HCV) and cirrhosis are major risk factors for HCC development [1, 2]. At present, HCC surveillance with tumor markers and imaging studies such as ultrasonography (US), computed tomography (CT), and magnetic resonance imaging (MRI) have been recommended for patients with cirrhosis [3, 4]. These imaging studies are expensive and the ultrasound is highly dependent on the ability of the operator. Therefore, more sensitive and specific serum biomarkers for early detection of HCC are desirable.

Serum tumor markers for detecting HCC could be divided into 4 categories: oncofetal and glycoprotein antigens, enzymes and isoenzymes, genes, and cytokines. Alpha-fetoprotein (AFP) and protein induced by vitamin-K absence or antagonist-II (PIVKA-II) also called des-gamma-carboxyprothrombin (DCP) are representative tumor markers for the diagnosis of HCC.

The elevated level of AFP is observed in only 50–70% of patients with HCC and also frequently in patients with cirrhosis or exacerbations of chronic hepatitis [5], and its sensitivity is low in patients with earlier/small tumors [6–8]. Measurement of lectin lens culinaris agglutinin (LCA) bound fraction of AFP (AFP-L3) can improve the specificity of AFP. Elevated DCP activity was only present in 28–47.6%

of HCCs of less than 3 cm in size [9–11]. Therefore, there has been growing interest and need to develop novel HCC serum biomarkers with greater sensitivity and specificity. Recent studies indicate that some other tumor markers, such as glypican 3 [12–17], gamma-glutamyl transferase II [18], alpha-1-fucosidase [19, 20], vascular endothelial growth factor [21–23], and transforming growth factor-beta 1 [24, 25] could serve as a complementary marker for AFP. Furthermore, the circulating genetic markers such as AFP-mRNA [26, 27] and human telomerase reverse transcriptase mRNA [28, 29] have been shown to be diagnostic and prognostic indicators of HCC.

Proteomics is the systematic study of proteomes, which describes the complete set or proteins found in a given cell type as well as of body fluids such as serum and urine. Recent advances in sophisticated technologies in proteomics should provide promising ways to discover novel markers in various fields of clinical medicine.

Increasing number of recent reports provide evidence that proteomic approach is promising tools to discover and identify novel biomarker for HCC. In particular, surface-enhanced laser desorption/ionization time-of-flight mass spectrometry (SELDI-TOF MS) is a representative example of a proteomics technique for the high-throughput fingerprinting of serum proteins and peptides [30]. We used the SELDI technology to generate comparative protein profiles of consecutive serum samples obtained during abstinence from alcoholic patients and found some novel biomarker for excessive alcohol consumption [31, 32]. Using this technique, several protein peaks leading to differentiation of patients with HCC from patients with cirrhosis alone have been discovered [33, 34]. In these studies, crude serum samples were directly analyzed without particular preanalytical preparations. The technical challenge in the analysis of serum proteome is that serum proteins are present at unequal concentrations. Indeed, 22 of the most abundant proteins account for >99% of total serum proteins [35], which hampers the detection of thousands of other low abundance proteins and peptides.

To detect the disease-associated proteins present in low abundance using currently available methods, the most abundant proteins have to be removed first by technique such as immunodepletion. We recently developed a three-step serum proteome analysis involving removal of 12 abundant proteins and subsequent reversed-phase high-performance liquid chromatography fractionation and one-dimensional electrophoresis and identified three proteins including YKL-50 as a promising biomarker of sepsis [36]. More recently, using this method, we identified promising biomarkers for alcohol abuse [37], breast cancer [38], and pancreatic cancer [39].

In this study, we applied this three-step proteome analysis to find novel biomarkers of HCC.

2. Material and Methods

2.1. Patients and Serum Samples. As an initial set of samples, blood samples of 12 HCV-related HCC patients and 10 HCV-related LC patients obtained at the Department of Medicine and Clinical Oncology, Chiba University Hospital, were used for comprehensive proteome analysis. All patients were positive for hepatitis C antibodies on the day of sampling and were diagnosed pathologically or clinically.

Diagnostic values of marker candidates identified in the initial set of samples were further validated using another set of samples. For this purpose, serum sample sets of 64 HCV-related HCC and 60 HCV-related LC patients were obtained from Chiba University Hospital and 60 healthy individuals for normal control from Kashiwado Clinic in Port-Square of Kashiwado Memorial Foundation, Chiba. These healthy individuals were defined in this study as subjects without medication on a regular basis, obesity, heavy drinking, abnormal liver test results, and hepatitis virus carriage.

Written informed consent was obtained from all patients. Serum samples were obtained and processed under the standardized conditions as we reported elsewhere [40] and were stored as aliquots at −80°C until analysis.

The clinical characteristics of all the patients are shown in Tables 1 and 2.

2.2. Immunoaffinity Depletion of High-Abundant Proteins from Human Serum. The outline of our experimental procedures is summarized in Figure 1. For removal of the twelve most abundant proteins: albumin, IgG, transferrin, fibrinogen, IgA, aplha2-macroglobrin, IgM, aplha1-antitrypsin, haptoglobin, aplha1-acidglycoprotein, apolipoprotein A-I, and apolipoprotein A-II, Proteome Lab IgY-12HC LC10 column (Beckman coulter Inc., Fullerton, CA, USA) was used. According to the manufacturer's instructions, 100 μL of each serum was diluted 5-fold with buffer A (dilution buffer) and injected onto the column in 100% buffer A at a flow rate of 0.5 mL/min for 25.0 min and 2.0 mL/min for 5.0 min on a Shimadzu LC10A VP system (Shimadzu Co., Kyoto, Japan). After collection of the flow-through fraction containing unbound proteins, the column was washed and the bound proteins were eluted with 100% buffer B (stripping buffer) at a flow rate of 2.0 mL/min for 18.0 min.

The chromatograms were monitored at 280 nm and 8 fractions (flow-through) were collected at 0.5 min intervals from 12.1 to 20.0 min. The fractions were collected into 1.5 mL microcentrifuge tubes.

2.3. Concentrating of Fractions by Centrifugal Ultrafiltration. The flow-through fractions (total 4.0 mL) were applied to Vivaspin 2 spin concentrators (MWCO 10 KD, Vivascience, Hannover, Germany) and concentrated to a volume of 80 μL according to the manufacturer's instructions. The concentrated pool was stored at −80°C until use.

2.4. HPLC Sample Preparation, Separation, and Fraction Collection. HPLC separations were performed on an automated SHISEIDO NANOSPACE SI-2 system (Shiseido Fine Chemicals, Tokyo, Japan). Injection was performed by an autosampler with a completely filled 100 μL injection loop. 75 μL of concentrated flow-through samples were directly loaded onto the Intrada WP-RP column (Imtakt, Kyoto,

Table 1: Clinical characteristics of the 12 HCC (a) and 10 LC (b) patients.

(a)

Case number	Sex	Age	Stage	Child-Pugh	Tumor size (mm)	Differentiation	AFP (ng/mL)	PIVKA-II (mAU/mL)
H1	M	71	III	A	Multiple, max 30	Poorly	70.6	18
H2	M	73	IV	B	Multiple, max 50	Moderately	549.6	44
H3	F	69	III	A	38	Moderately–well	11.9	59
H4	M	73	III	B	32–30	Moderately	208.1	20
H5	M	69	III	B	29–25	Moderately–well	38.3	12
H6	F	77	III	A	Multiple, max30	Moderately–well	47.3	10
H7	M	67	III	A	30–10	Moderately	14.9	35
H8	F	71	III	B	35–20	Well	1031.7	466
H9	M	58	IV	B	20	Moderately	25.1	75
H10	F	71	III	B	30	Poorly–moderately	14640	<10
H11	M	81	III	A	25	Moderately	62.3	6854
H12	M	70	III	A	60	—	1390	5350

(b)

Case number	Sex	Age	Child-Pugh	AFP (ng/mL)	PIVKA-II (mAU/mL)
L1	M	45	B	12	—
L2	F	54	A	36.4	<10
L3	M	59	A	24.3	31
L4	M	59	B	12.8	66
L5	F	62	A	4.5	—
L6	M	43	A	8.5	—
L7	M	48	B	11.3	—
L8	M	60	A	37.7	—
L9	F	68	A	15.3	—
L10	M	45	B	6	—

Table 2: Clinical characteristics of 64 patients with HCC, 60 with LC and 60 normal control subjects.

	HCC	LC	Normal control
	$n = 64$	$n = 60$	$n = 60$
Age, mean ± SD	66.1 ± 9.9	56.8 ± 12.3	54.5 ± 7.0
Male/female	7.0	6.5	6.5
AFP level (ng/mL), mean ± SD	1926.2 ± 11904.7	14.7 ± 24.2	3.5 ± 1.6
PIVKA-II level (mAu/mL), mean ± SD	11757.2 ± 50071.5	18.1 ± 12.5	19.71 ± 5.4

Japan). The RP separations for each flow-through were performed under a set of conditions using a multisegment elution gradient, with eluent A (0.1% TFA in water, v/v) and eluent B (0.08% TFA in 90% acetonitrile, v/v). The gradient conditions consisted of three steps with increasing concentrations of the eluent B: 5% B 5 min, 5–95% B 23 min, 95% B 11 min, and 5% B 21 min for reequilibration of the column, at a flow rate of 0.40 mL/min for a total runtime of 60 min.

The chromatograms were monitored at 218 nm and 40 fractions were collected at 0.5 min intervals from 19.1 to 39.1 min. Each fraction was dried in a centrifugal vacuum concentrator and stored at −80°C for subsequent SDS-PAGE analysis.

2.5. Electrophoretic Analysis. Dried fraction samples from HPLC separations were dissolved in 15 μL of sample preparation buffer, vortexed, and then loaded onto the two Perfect NT Gels (10–20% acrylamide, 20 wells, 140 mm × 140 mm × 1 mm; DRC. Co., Ltd.).

SDS-PAGE analysis was carried out by an established method [41]. Following electrophoresis, proteins were visualized by silver staining using 2D silver stain II "DAIICHI" (Daiichi Pure Chemicals Co., Ltd., Osaka, Japan).

2.6. In-Gel Digestion. For protein identification, samples were prepared again as described above. To obtain high sensitivity, the same process was repeated three times per sample; finally dried fraction sample of triple amount were obtained. 45 μL of combined dried fraction samples were loaded on to SDS-PAGE gel as described above after these samples were individually dissolved with 15 μL sample buffer.

After then, protein spots in Coomassie brilliant blue (CBB) stained SDS-PAGE gels were individually excised in squares of about 1 to 2 mm per side destained in 50% v/v acetonitrile/50 mM NH_4HCO_3 and then washed with

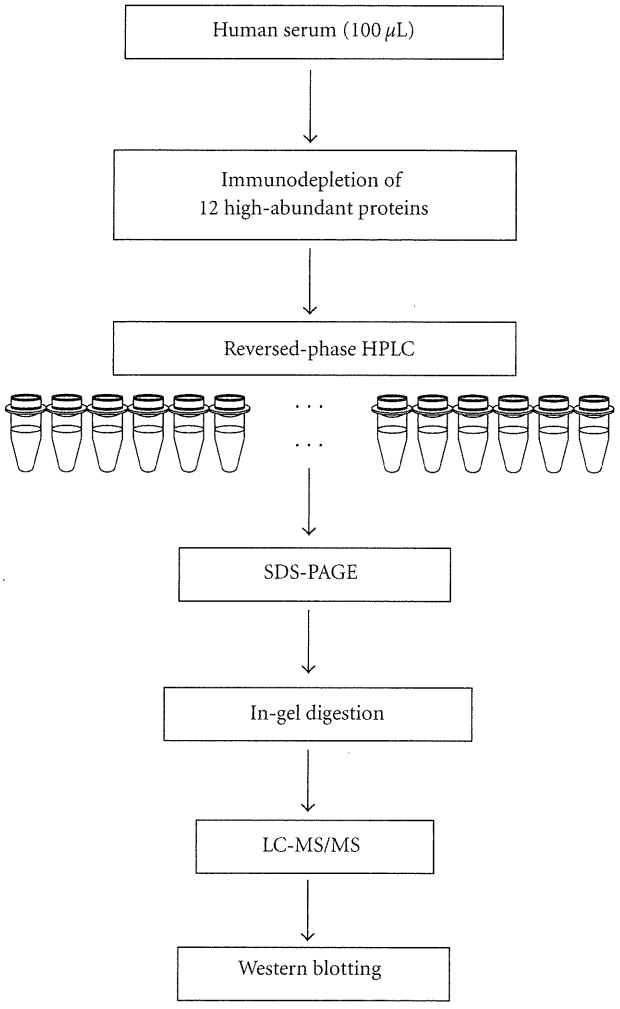

FIGURE 1: Schematic diagram of the experimental protocol.

deionized water. The gel pieces were dehydrated in 100% acetonitrile for about 15 min and then dried in a SpeedVac Evaporator (Wakenyaku, Kyoto, Japan) for 60 min. The pieces were rehydrated in 10–20 μL of 25 mM Tris-Cl (pH 9.0) containing 25 ng/μL trypsin (Trypsin sequence grade, Roche, Mannheim, Germany) for 45 min at 4°C. After removal of excess trypsin, the gel pieces were incubated in a minimal volume (10–20 μL) of 50 mM Tris (pH 9.0) buffer for 24 h at 37°C. The solution containing digested fragments of proteins was transferred to 1.5 mL siliconized plastic test tube and stored at 4°C. Peptide fragments remaining in gel pieces were further recovered after 20 min incubations at room temperature in minimal volumes of 5% v/v formic acid containing 50% v/v acetonitrile. The solutions containing peptides were pooled together in the tube at 4°C.

2.7. LC-MS/MS. Molar quantities of recovered peptide fragments were estimated from the staining intensity of the SDS-PAGE bands that were digested in-gel with trypsin. Digested peptides equivalent to the maximum of 10 pmoL of a protein in an SDS-PAGE band were injected into a Magic C18 column (Michrom Bioresources, Inc., CA, USA), which was attached to the MAGIC 2002 (Michrom Bioresources, Inc., CA, USA) high-performance liquid chromatography (HPLC) system. The flow rate of the mobile phase was 1 μL/min using MAGIC Variable Splitter. The solvent composition of the mobile phase was programmed to change in 50 min cycles with varying mixing ratios of solvent A (2% v/v CH_3CN and 0.1% v/v HCOOH) to solvent B (90% v/v CH_3CN and 0.1% v/v HCOOH). Next, the peptides were eluted with a linear gradient from 0 to 50% solvent B. Purified peptides were introduced from HPLC to Q-star (Applied Biosystems, Foster City, CA, USA), a hybrid quadrupole time-of-flight mass spectrometer, via an attached FortisTip (AMR, Tokyo, Japan). Mascot search engine (Matrixscience, London, UK) was used to identify proteins from the mass and tandem mass spectra of peptides. Peptide mass data were matched by searching the National Center for Biotechnology Information database using MASCOT engine (http://www.matrixscience.com/). The minimum criterion of the probability-based MASCOT/MOWSE score was set with 5% as the significant threshold level.

2.8. Western Blot Analysis. After the 12 abundant proteins were removed from serum as described above, the depleted samples were separated on SDS-polyacrylamide gel electrophoresis (80 × 40 × 1.0 mm, 10–20% polyacrylamide gradient gel, 240 V) and transferred to a methanol-rinsed polyvinyl-difluoride (PVDF) membrane (0.45 μm pore size in roll form, Millipore, Bedford, MA) (Amersham, Hybond-C Extra Supported) (40 V, 25 min) using the XV Pantera System (DRC Co., Ltd., Tama, Japan). After transferring the proteins to a membrane and blocking with 5% skim milk in phosphate-buffered saline (PBS) for 1 h at room temperature, the membranes were incubated at 4°C overnight with the primary antibody to clusterin (1 : 3000, mouse monoclonal, upstate (now part of Millipore), CA, USA). The membrane was washed for a total 30 min in 3 changes of PBS-Tween (0.1%) prior to incubation in the appropriate horseradish peroxidase-linked secondary antibody (anti-mouse IgG horseradish peroxidase-linked secondary antiserum, 1 : 500) for 1 h at room temperature. The membranes were finally washed three times as previously described, and immunoreactive proteins were revealed with an enhanced chemiluminescence substrate reaction using ECL western blotting detection reagents (GE Healthcare UK Ltd., Amersham, England) according to the manufacturer's instructions.

2.9. Gel Imaging and Analysis. The Silver-stained SDS-gels and CBB-stained gels were scanned with an optical resolution of 400 dpi by EPSON ES-2000 scanner (SEIKO EPSON Corp., Nagano, Japan) using EPSON TWAIN Pro software (SEIKO EPSON Corp., Nagano, Japan). The images were processed using Photoshop 6 (Adobe) software. After scanning, each gel was stored at 4°C.

TIFF files of the gel images were transferred for analysis with a TotalLab TL120 (Nonlinear Dynamics Ltd., Newcastle, UK) and were used for band detection and statistical analysis.

2.10. Measurement of Serum Clusterin Concentration by ELISA. Serum clusterin was quantified using a human clusterin ELISA kit (R&D systems, Inc., MN, USA) following manufacturer's instructions. Human clusterin standard as provided in the kit (1,000 ng/mL: stock solution), and the serially diluted standards (200–3.12 ng/mL) were prepared from the stock solution. Calibrator Diluent RD5T (dilution buffer) serves as the blank. Test serum samples were diluted 1 : 2000 in the dilution buffer.

After adding 100 μL of Assay Diluent RD1-19 to each well, 50 μL aliquots of the standards and diluted test samples were added in duplicate to the wells of a microtiter plate coated with antihuman clusterin antibody.

After incubation at room temperature for 2 hours on a horizontal orbital shaker, the plate was washed using 400 μL of Wash Buffer and repeated three time processes and a total of four washes. After the last wash, 200 μL of antihuman clusterin monoclonal antibody conjugated to horseradish peroxidase was added to the wells. The plate was incubated for 2 hours at room temperature on the shaker, followed by washes as before and addition of 200 μL of substrate solution containing hydrogen peroxide and tetramethylbenzidine to the wells. The plate was stetted at the dark to protect from light and incubated for 30 min at room temperature to allow for color development. The reaction was stopped by the addition of 50 μL of stop solution, and the optical densities were determined by reading absorbance at 450 nm with iMark Microplate Reader (Bio-Rad Laboratories, Inc., CA, USA).

2.11. Other Procedures. Numerical data were presented as mean ± SD. Statistical significance of difference was assessed by Student's t-test; P values less than 0.05 were considered significant.

Serum AFP and PIVKA-II levels were determined by commercially available assay kits.

3. Results

3.1. Immunoaffinity Serum Depletion. Schematic diagram of our experimental protocol is summarized in Figure 1.

Figure 2 is a representative immunoaffinity chromatogram and shows a substantial removal of high-abundant proteins from a human serum sample. The immunodepletion of the high-abundant serum proteins was conducted in a reproducible manner in samples obtained from seven HCC and five LC patients (data not shown). A total of 4 mL of flow-through fractions were collected, desalted, and concentrated prior to reversed-phase HPLC.

3.2. RP-HPLC. Figure 3 is a representative reversed-phase HPLC chromatogram. Forty fractions were collected every 0.5 minute from 19.1 to 39.1 minutes (Figure 3(a), arrow). Fractions numbers 1–5, numbers 6–8, numbers 26–30, numbers 31–35, and numbers 36–40 were pooled, respectively, since protein concentration of each fraction was apparently very low. Therefore, a total of 22 fractions were processed for SDS-PAGE analysis (Figure 3(b)).

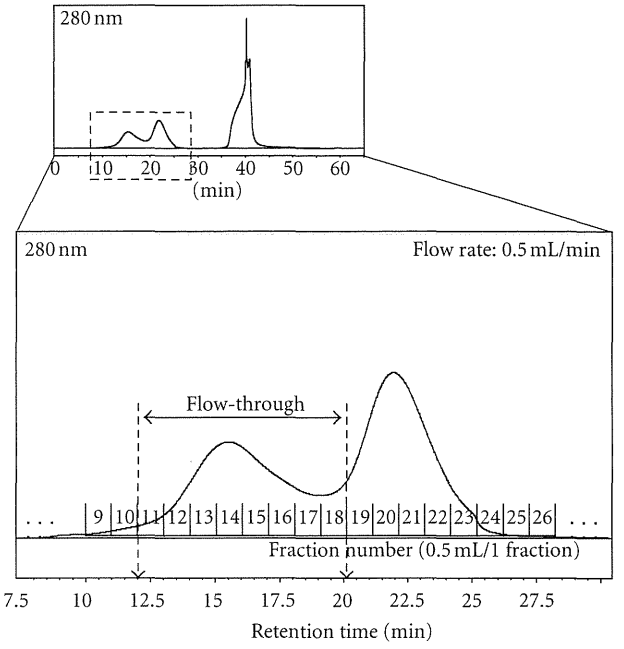

FIGURE 2: Representative chromatogram during removal of highly abundant serum proteins by an immunoaffinity column. 100 μL of serum (diluted fivefold) was injected on the immunoaffinity column and was eluted (0.5 mL/min) as described in the experimental procedures. Flow-through fractions (12.1–20.0 min) were collected, and then a total of 4.0 mL fractions were concentrated to a volume of 80 μL using Vivaspin 2 for reversed-phase HPLC fractionation.

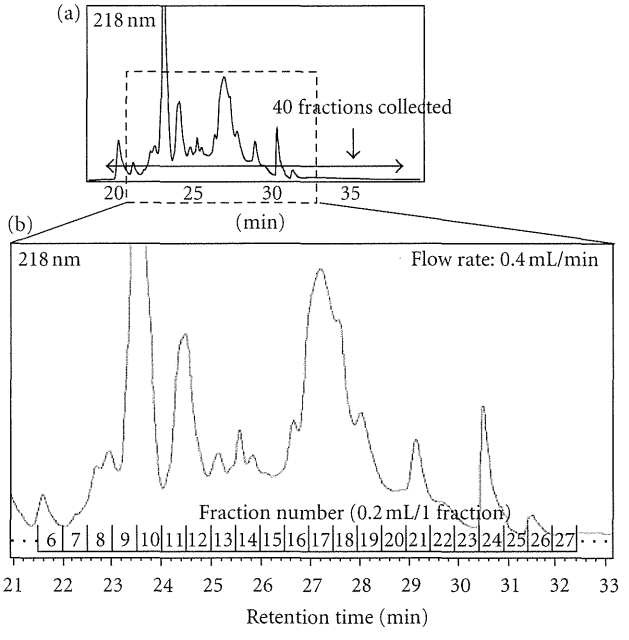

FIGURE 3: Representative chromatogram during fractionation by RP-HPLC of serum samples in which highly abundant proteins were immunodepleted. Concentrated immunodepleted samples were directly loaded onto the RP column and 40 fractions were collected every 0.5 min from 19.1 to 39.1 min ((a) arrow) as described in the experimental procedures. Among them, a total of 22 fractions were processed for SDS-PAGE analysis (b).

TABLE 3: Upregulated proteins identified by LC-MS/MS in human HCC serum. Details are described in the experimental procedures.

Protein name	Theoretical mass	Experimental mass	Score	Coverage	Queries matched
Afamin precursor	69024	90000	563	23%	16
Alpha-1-antichymotrypsin	48606	95000	118	4%	2
Alpha-1-B-glycoprotein	51908	95000	88	5%	2
Alpha-1-microglobulin	16531	230000	99	15%	2
Alpha-2-macroglobulin	163175	170000	2465	34%	76
Angiotensinogen	53122	55000	705	29%	23
Antithrombin III	49008	62000	389	24%	9
Apolipoprotein A-IV	45307	43000	639	30%	12
Apolipoprotein B	187126	140000	332	4%	7
Apolipoprotein B-100	515077	140000	267	1%	5
Apolipoprotein E	36185	35000	832	44%	33
Beta-actin	41710	41000	226	17%	4
C1q	26442	33000	113	11%	2
C2 precursor	83214	97000	557	15%	14
C3	187046	180000	613	7%	11
C3b	103886	120000	2042	26%	63
C3c	187046	33000	206	2%	4
C3d	120000	187046	153	1%	3
C3, isoform CRA_a	70000	143619	1636	28%	64
C4A	192741	24000	456	5%	21
C4B	40737	41000	138	7%	2
C5	141723	120000	248	4%	6
C6	104776	120000	96	4%	2
C7	93449	95000	874	22%	27
C8-alpha subunit	65111	55000	109	3%	2
C8-beta propeptide	62008	70000	323	11%	7
C8-gamma polypeptide	22206	23000	352	40%	15
C9	60359	70000	496	14%	12
Complement receptor type 2 (Cr2)	112900	160000	160	2%	2
Component factor B	85450	50000	163	4%	3
Cr2-C3d complex	34437	35000	151	10%	3
Complement component (3b/4b) receptor 1	61415	160000	102	4%	2
Carbonic anhydrase I	28852	25000	195	18%	4
Carbonic anhydrase II	29200	33000	208	18%	4
Carboxypeptidase N Polypeptide 1 precursor	52253	45000	147	11%	3
Carboxypeptidase N precursor	60578	97000	330	11%	6
Cathepsin D preproprotein	44524	49000	103	6%	2
Cationic trypsinogen	160000	120901	66	—	2
CD14 protein precursor	40111	55000	365	21%	8
Ceruloplasmin	115398	140000	1520	27%	44
Clusterin	48772	39000	95	8%	2
C-type lectin domain family 3, member B	22552	25000	243	24%	6
Fibronectin precursor	256529	230000	176	2%	3
Galectin 3 binding protein	65289	90000	177	3%	3
Gelsolin	85644	95000	474	15%	11
Glutathione peroxidase 3 precursor	25489	26000	167	16%	4
Hemopexin precursor	51512	50000	104	4%	2

Table 3: Continued.

Protein name	Theoretical mass	Experimental mass	Score	Coverage	Queries matched
Heparin cofactor II	57034	110000	372	21%	8
Insulin-like growth factor binding protein	65994	95000	176	6%	3
Interalpha-trypsin inhibitor heavy chain H1	101339	230000	631	14%	23
Interalpha-trypsin inhibitor heavy chain H2	106370	230000	862	15%	28
ITI family heavy chain-related protein	103321	120000	348	9%	6
Kininogen 1	47853	120000	355	13%	7
Lactate dehydrogenase B	36615	35000	217	13%	4
Leucine-rich alpha-2-glycoprotein 1	38154	50000	301	15%	8
Lumican	38375	70000	320	21%	7
M130 antigen	160000	120901	66	1%	2
Multimerin 2	104352	20000	88	1%	2
Pancreatic carboxypeptidase A1 precursor	47111	41000	92	5%	2
Peptidoglycan recognition protein 2 precursor	67927	70000	96	7%	2
Pigment epithelial-differentiating factor (serpin-F1)	46313	48000	946	50%	22
Plasma protease (C1) inhibitor precursor	55147	90000	829	25%	43
Prepro-plasma carboxypeptidase B	48411	62000	100	6%	2
Preserum amyloid P component	25381	30000	362	26%	13
Prolidase	54348	55000	82	3%	2
Proteasome alpha 4 subunit isoform 1	29465	33000	85	8%	2
Sex-hormone-binding globulin	43768	45000	391	28%	10
Thyroxine-binding globulin precursor	46295	55000	135	6%	3
Trypsin inhibitor	106647	55000	174	5%	3
Vascular cell adhesion molecule 1 isoform	81224	97000	133	3%	2
Vitamin D binding protein	51183	55000	669	21%	17
Vitamin K-dependent protein S	75074	95000	106	3%	2
Vitronectin	54308	10000	90	2%	2

3.3. SDS-PAGE Analysis. The representative silver-stained SDS-PAGE gel of a fraction (fraction number 13) obtained from seven HCC patients and five LC patients is shown in Figure 4(a).

Comparison of SDS-PAGE patterns of a total of 22 fractions revealed that intensities of 83 bands were greater in more than 3 cases of HCC than in those in LC cases. Among these, the intensities of 14 bands were increased in all the seven HCC patients. The representative examples are indicated by arrow heads.

3.4. Identification of Protein. To identify proteins, the expression of which was different between HCC and LC on silver stained gel, four HCC and four LC sera were fractionated and separated using SDS-PAGE again, and then gels were stained by CBB (Figure 4(b)). Because the sensitivity of the CBB stain is lower than of the silver stain, samples for identification were prepared from the beginning by repeating three courses of the procedures, from depletion of the major proteins to RP-HPLC fractionation. As a result, additional 71 bands were found to have altered intensity levels between the two groups on CBB gels. Thus, a total of 154 bands were considered as initial candidate bands. Forty-six out of these 154 bands, derived from more than two adjacent fractions, were not processed further. Finally, 108 bands were subjected to in-gel trypsin digestion: among them 73 proteins were identified by LC-MS/MS (Table 3 and Figure 5).

3.5. Western Blotting. Western blotting analysis could confirm that clusterin was overexpressed in the majority of HCC sera as compared with LC (Figure 6(a)).

Semiquantitative analysis of the results by TotaLab TL120 (Shimadzu Co., Ltd., Kyoto) revealed that the difference in serum clusterin levels between HCC and LC was statistically significant (468211.38 ± 103972.69 versus 341686.90 ± 123162.85, $P = 0.023$) as indicated in Figure 6(b).

3.6. Clusterin Concentration in Serum from HCC and LC Patients. To evaluate diagnostic values of serum clusterin levels for HCC diagnosis, we examined sera from 64 patients with HCC, 60 with LC, and 60 normal subjects. The concentration of clusterin (mean ± SD) was $210.4 \pm 61.3\,\mu$g/mL for HCC, $170.9 \pm 50.0\,\mu$g/mL for LC, and $139.4 \pm 37.4\,\mu$g/mL for normal subjects and was significantly higher in HCC than in LC ($P < 0.01$, Student's t-test) and in normal subjects ($P < 0.001$) (Figure 7).

We set the cut-off value of clusterin at $230\,\mu$g/mL by calculating the mean + 2 SD of healthy 60 samples. As a result, clusterin level above the value was found in 23 of 64 HCCs (35.9%) and in 6 of 60 LCs (10.0%). Furthermore,

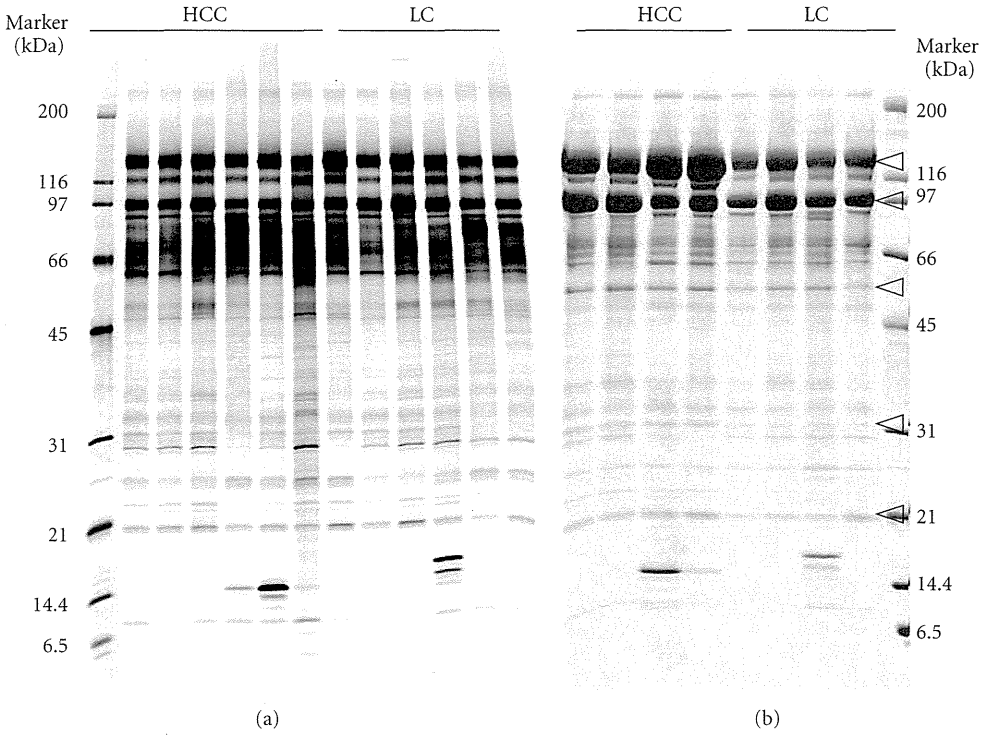

FIGURE 4: Representative SDS-PAGE pattern of immunodepleted serum sample after RP-HPLC fractionation (fraction number 13). 100 μL of serum samples from seven HCC patients and five LC patients was immunodepleted and injected onto the column. Forty fractions were collected and dried, and among them 22 fractions were separated using 10–20% SDS-PAGE. Each dried fraction was dissolved in 15 μL of sample buffer and loaded onto the gel as described in the experimental procedures. Following electrophoresis, proteins were visualized by silver staining (a). For protein identification, 300 μL of serum samples was prepared again and visualized by CBB staining (b). The intensities of 14 bands were increased in all the seven HCC patients. The representative examples are indicated by arrow heads.

MSNQGSKYVN KEIQNAVNGV KQIKTLIEKT NEERKTLLSN LEEAKKKKED
ALNETRESET KLKELPGVCN ETMMALWEEC KPCLKQTCMK FYARVCRSGS
GLVGRQLEEF LNQSSPFYFW MNGDRIDSLL ENDRQQTHML DVMQDHFSRA
SSIIDELFQD RFFTREPQDT YHYLPFSLPH RRPHFFFPKS RIVRSLMPFS
PYEPLNFHAM FQPFLEMIHE AQQAMDIHFH SPAFQHPPTE FIREGDDDRT
VCREIRHNST GCLRMKDQCD KCREILSVDC STNNPSQAKL RR**ELDESLQV**
AERLTRKYNE LLKSYQWKML NTSSLLEQLN EQFNWVSRLA NLTQGEDQYY
LR**VTTVASHT** **SDSDVPSGVT** **EVVVK**LFDSD PITVTVPVEV SRKNPKFMET
VAEKALQEYR KKHREE

FIGURE 5: Identification of clusterin by LC-MS/MS. The amino acid sequence of clusterin is shown. Matched peptide sequences are printed in bold and underlined.

serum clusterin levels were above the cut-off value in 5 of 12 HCCs (41.7%) in whom both serum AFP and PIVKA-II were within their cut-off values, suggesting that clusterin is complementary to the conventional two representative HCC tumor markers.

4. Discussion

The sequencing of the human genome has opened the door for comprehensive transcriptome and proteome analysis. Transcriptome analyses have revealed unique patterns for gene expression that are clinically informative. Messenger RNA abundances, however, are not necessarily predictive of corresponding protein abundances [42]. Since the detailed understanding of biological processes, both in healthy and pathological states, requires the direct study of relevant proteins, proteomics bridges the gap between the information coded in the genome sequence and cellular behavior. Therefore, proteomics is among the most promising technologies for the development of novel diagnostic tools.

Increasing number of studies has taken advantage of various proteomic technologies to discover and identify

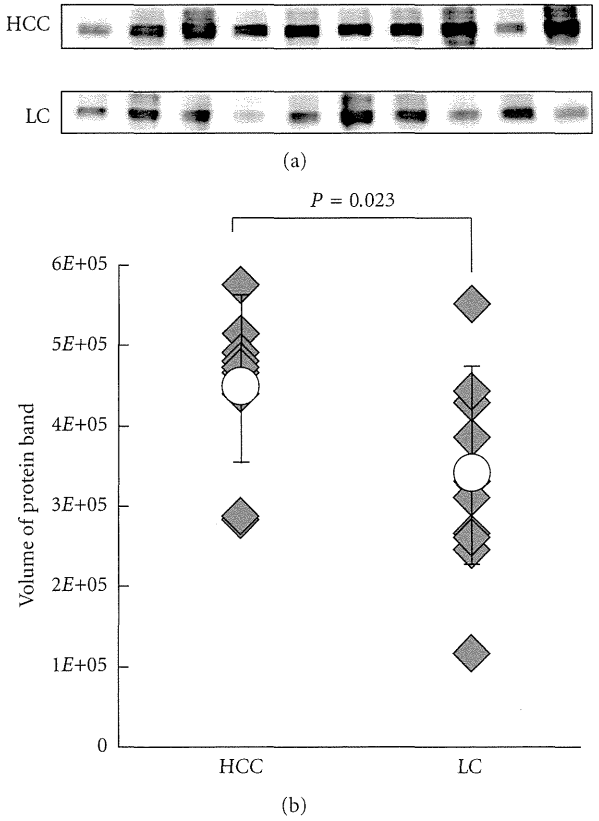

FIGURE 6: Western blot analysis of clusterin in sera from HCC and LC groups. (a) Immunoedpleted sera of the 5 HCC and 5 LC SDS-PAGE cases and additional 5 HCC and 5 LC cases were separated by 10.0–12.0% SDS-PAGE and probed with anticlusterin. The expression levels are relatively higher in the HCC groups than LCs. (b) Differences in expression were analyzed by the Student's t-test. The expression levels of these proteins were upregulated significantly in HCC samples ($P = 0.023$). Rhombuses represent volumes of individual samples. Line indicates the range with the open circles indicating the mean values.

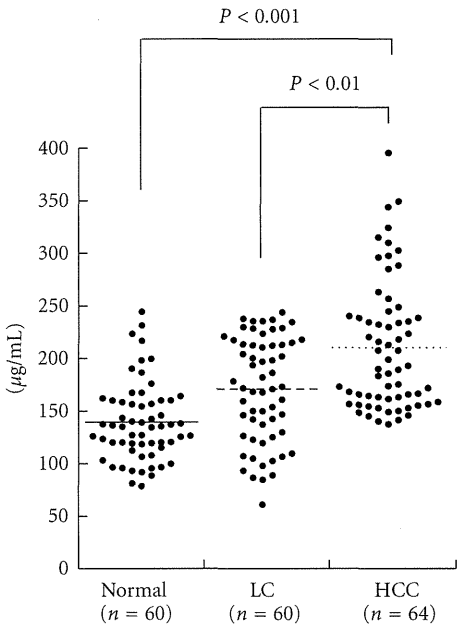

FIGURE 7: Concentration of clusterin in 64 patients with HCC, 60 patients with LC and 60 healthy individuals. Clusterin levels, quantified using ELISA, were significantly greater in HCC patients compared with LC, ($P < 0.01$) and normal subjects ($P < 0.001$).

novel HCC markers. Clinical tissue samples have been the most extensively studied samples in HCC proteomic studies. Most studies compared protein expression profiles between tumor tissues and adjacent nontumor tissues using two dimensional electrophoresis (2DE) and two dimensional fluorescence difference gel electrophoresis (2D-DIGE).

Some studies used laser capture microdissection (LCM) in order to characterize isolated tumor cell populations from heterogeneous tissue sections. By combing LCM and 2D-DIGE, Liang et al [43]. found that the protein profiles of well- and poorly differentiated HCC tissues are significantly different. Proteome analyses of tumor tissues should be a basis for HCC marker discovery and a number of proteins have been identified as candidate markers for HCC [44–46]; none of them have been shown to be useful serum marker in a clinical setting. Among thousands of serum proteins and peptides, a few are so dominant that they may hamper the detection of other low abundance proteins or peptides. To overcome this problem, Feng et al. [47] took a strategy to deplete abundant proteins such as albumin and immunoglobulin before analyses, followed by 2DE and MALDI-TOF MS/MS identification. They showed that heat-shock-protein 27 could aid in the diagnosis of HCC.

In this study, three-step procedures including the immunodepletion of 12 abundant proteins were carried out to discover novel HCC markers. As a first step, serum samples were subjected to antibody-based immunoaffinity column that simultaneously removes 12 abundant serum proteins. The concentrated flow-through was then fractionated using reversed-phase HPLC. Proteins obtained in each HPLC fraction were further separated by SDS-PAGE. A total of 73 differentially expressed proteins were identified and among them clusterin was of particular interest as potential serum marker for HCC and differences in this expression in serum were confirmed by the western blotting.

Further validation using another set of serum sample set showed that clusterin level was significantly higher in HCC than in LC as determined by ELISA. It is notable that serum clusterin levels were elevated in 5 out of 12 HCC cases in which both AFP and PIVKA-II were within their cut-off values. As a result, combination assays of AFP PIVKA-II and clusterin could detect about 90% of HCC cases included in this study. These result suggested that clusterin could be HCC tumor marker complemenatary to AFP and PIVKA-II.

Clusterin, also known as apolipoprotein J (Apo J), sulfated glycoprotein 2, is a heterodimeric glycoprotein present in most animal tissues and body fluids [48]. This glycoprotein plays important roles in a variety of physiological processes including lipid transport [49], reproduction [50], tissue remodeling [51], and senescence [52].

Clusterin overexpression has been shown in various human malignancies including cancer of the breast [53], pancreas [54], and colon [55]. Kang et al. [56] demonstrated the overexpression of clusterin in HCC and suggested that its cytoplasmic overexpression might be a predictor of poor survival. Increased serum levels of clusterin in HCC patients had not been reported before.

In conclusion, the results of this study suggest that clusterin can be a supplementary serum biomarker for HCC. Exact mechanisms and pathophysiological significance for the upregulation of clusterin in HCC remain to be investigated. Furthermore, since the majority of HCC cases in Japan are related to HCV, we focused on HCV-related HCC in the present study. It will be necessary to assess diagnostic values of serum clusterin levels in HBV-related cases as well.

List of Abbreviations

HCC: Hepatocellular carcinoma
AFP: Alpha-fetoprotein
DCP: Des-gamma-carboxy prothrombin
LC: Liver cirrhosis
SDS-PAGE: Sodium dodecyl sulfate polyacrylamide gel electrophoresis.

References

[1] J. O. Ogunbiyi, "Hepatocellular carcinoma in the developing world," *Seminars in Oncology*, vol. 28, no. 2, pp. 179–187, 2001.

[2] L. J. Lopez and J. A. Marrero, "Hepatocellular carcinoma," *Current Opinion in Gastroenterology*, vol. 20, no. 3, pp. 248–253, 2004.

[3] S. Fujiyama, M. Tanaka, S. Maeda, H. Ashihara, R. Hirata, and K. Tomita, "Tumor markers in early diagnosis, follow-up and management of patients with hepatocellular carcinoma," *Oncology*, vol. 62, no. 1, pp. 57–63, 2002.

[4] J. Szklaruk, P. M. Silverman, and C. Charnsangavej, "Imaging in the diagnosis, staging, treatment, and surveillance of hepatocellular carcinoma," *American Journal of Roentgenology*, vol. 180, no. 2, pp. 441–454, 2003.

[5] P. J. Johnson, "The role of serum alpha-fetoprotein estimation in the diagnosis and management of hepatocellular carcinoma," *Clinics in Liver Disease*, vol. 5, no. 1, pp. 145–159, 2001.

[6] D. S. Chen, J. L. Sung, and J. C. Sheu, "Serum α-fetoprotein in the early stage of human hepatocellular carcinoma," *Gastroenterology*, vol. 86, no. 6, pp. 1404–1409, 1984.

[7] F. Trevisani, S. De Notariis, G. Rapaccini et al., "Semiannual and annual surveillance of cirrhotic patients for hepatocellular carcinoma: effects on cancer stage and patient survival (Italian experience)," *American Journal of Gastroenterology*, vol. 97, no. 3, pp. 734–744, 2002.

[8] F. Nomura, K. Ohnishi, and Y. Tanabe, "Clinical features and prognosis of hepatocellular carcinoma with reference to serum alpha-fetoprotein levels: analysis of 606 patients," *Cancer*, vol. 64, no. 8, pp. 1700–1707, 1989.

[9] S. L. Tsai, G. T. Huang, P. M. Yang, J. C. Sheu, J. L. Sung, and D. S. Chen, "Plasma des-γ-carboxyprothrombin in the early stage of hepatocellular carcinoma," *Hepatology*, vol. 11, no. 3, pp. 481–488, 1990.

[10] K. Soga, T. Watanabe, K. Aikawa, M. Toshima, K. Shibasaki, and Y. Aoyagi, "Serum des-gamma-carboxyprothrombin level by a modified enzyme immunoassay method in hepatocellular carcinoma: clinical significance in small hepatocellular carcinoma," *Hepato-Gastroenterology*, vol. 45, no. 23, pp. 1737–1741, 1998.

[11] F. Nomura, M. Ishijima, K. Kuwa, N. Tanaka, T. Nakai, and K. Ohnishi, "Serum des-gamma-carboxy prothrombin levels determined by a new generation of sensitive immunoassays in patients with small-sized hepatocellular carcinoma," *American Journal of Gastroenterology*, vol. 94, no. 3, pp. 650–654, 1999.

[12] M. Capurro, I. R. Wanless, M. Sherman et al., "Glypican-3: a novel serum and histochemical marker for hepatocellular carcinoma," *Gastroenterology*, vol. 125, no. 1, pp. 89–97, 2003.

[13] Y. Hippo, K. Watanabe, A. Watanabe et al., "Identification of soluble NH2-terminal fragment of glypican-3 as a serological marker for early-stage hepatocellular carcinoma," *Cancer Research*, vol. 64, no. 7, pp. 2418–2423, 2004.

[14] T. Nakatsura, Y. Yoshitake, S. Senju et al., "Glypican-3, overexpressed specifically in human hepatocellular carcinoma, is a novel tumor marker," *Biochemical and Biophysical Research Communications*, vol. 306, no. 1, pp. 16–25, 2003.

[15] Y. Midorikawa, S. Ishikawa, H. Iwanari et al., "Glypican-3, overexpressed in hepatocellular carcinoma, modulates FGF2 and BMP-7 signaling," *International Journal of Cancer*, vol. 103, no. 4, pp. 455–465, 2003.

[16] Y. K. Sung, S. Y. Hwang, M. K. Park et al., "Glypican-3 is overexpressed in human hepatocellular carcinoma," *Cancer Science*, vol. 94, no. 3, pp. 259–262, 2003.

[17] Z. L. Lü, D. Z. Luo, and J. M. Wen, "Expression and significance of tumor-related genes in HCC," *World Journal of Gastroenterology*, vol. 11, no. 25, pp. 3850–3854, 2005.

[18] R. Cui, J. He, F. Zhang et al., "Diagnostic value of protein induced by vitamin K absence (PIVKAII) and hepatoma-specific band of serum gamma-glutamyl transferase (GGTII) as hepatocellular carcinoma markers complementary to α-fetoprotein," *British Journal of Cancer*, vol. 88, no. 12, pp. 1878–1882, 2003.

[19] P. Tangkijvanich, P. Tosukhowong, P. Bunyongyod et al., "alpha-L-fucosidase as a serum marker of hepatocellular carcinoma in Thailand," *Southeast Asian Journal of Tropical Medicine and Public Health*, vol. 30, no. 1, pp. 110–114, 1999.

[20] H. Ishizuka, T. Nakayama, S. Matsuoka et al., "Prediction of the development of hepato-cellular-carcinoma in patients with liver cirrhosis by the serial determinations of serum alpha-L-fucosidase activity," *Internal Medicine*, vol. 38, no. 12, pp. 927–931, 1999.

[21] Z. Liu, L. Yan, T. Xiang, L. Jiang, and B. Yang, "Expression of vascular endothelial growth factor and matrix metalloproteinase-2 correlates with the invasion and metastasis of hepatocellular carcinoma," *Sheng Wu Yi Xue Gong Cheng Xue Za Zhi*, vol. 20, no. 2, pp. 249–254, 2003.

[22] G. W. Huang, L. Y. Yang, and W. Q. Lu, "Expression of hypoxia-inducible factor 1α and vascular endothelial growth factor in hepatocellular carcinoma: impact on neovascularization and survival," *World Journal of Gastroenterology*, vol. 11, no. 11, pp. 1705–1708, 2005.

[23] S. J. Kim, I. K. Choi, K. H. Park et al., "Serum vascular endothelial growth factor per platelet count in hepatocellular carcinoma: correlations with clinical parameters and survival," *Japanese Journal of Clinical Oncology*, vol. 34, no. 4, pp. 184–190, 2004.

[24] B. C. Song, Y. H. Chung, J. A. Kim et al., "Transforming growth factor-β1 as a useful serologic marker of small hepatocellular carcinoma," *Cancer*, vol. 94, no. 1, pp. 175–180, 2002.